*Research Article*

# Analytical solution of Velocities and Temperature fields using Homotopy Analysis Method

**Dr. K.V.Tamil Selvi [1], M.Rajaram[2],Dr.A.Meena[3]**

[1] Department of Mathematics,Kongu Engineering College, Perundurai, Erode, Tamil Nadu, India.
e-mail : kvtamilselvi@gmail.com
[2]Ramanujan Research Centre in Mathematics, Saraswathi Narayanan College (Autonomous), Perungudi, Madurai, Tamil Nadu, India.
e-mail : rajaram23292@gmail.com
[3] Ramanujan Research Centre in Mathematics, Saraswathi Narayanan College (Autonomous), Madurai, Tamil Nadu, India. e-mail : meensphd@gmail.com
**Article History**:Received:11 January 2021; Accepted: 27 February 2021; Published online: 5 April 2021

**Abstract:** In this paper, analysis of nonlinear partial differential equations on velocities and temperature with convective boundary conditions are investigated. The governing partial differential equations are transformed into ordinary differential equations by applying similarity transformations. The system of nonlinear differential equations are solved using Homotopy Analysis Method (HAM). An analytical solution is obtained for the values of Magnetic parameter $M^2$, Prandtl number Pr, Porosity parameter $\lambda$, Radiation parameter R, Biot number Bi, Stretching parameter c. The present results are compared with the numerical result [1], showing good agreement with each other and with different parameters. The influence of the skin friction and local Nusselt number for different parameters are discussed. The effects of various parameters on velocity and temperature profiles are presented graphically.

**Keywords**: Mixed Boundary Conditions, Similarity Transformations, Homotopy Analysis Method, Skin friction Co-efficient, SCILAB

## 1. INTRODUCTION

S. Shaw et.al [1] explained the study of Magnetohydrodynamic (MHD) flow 3D casson fluid. It has many industrial applications, such as purification of crude oil, Magnetohydrodynamic electrical power generation [1]. Many authors [2-5] have been investigated experimentally and numerically for the MHD flow of Casson fluid with convective boundary conditions..

The main objective of this paper is to investigate the analytical solution of boundary layer flow of electrically conducting Casson fluid past. The

system of nonlinear partial differential equations has been diminished into the system of nonlinear ordinary differential equation [6-8]. S. Shaw et.al [1] presented the numerical solution of 3D Casson fluid flow using Spectral relaxation method. Still now there is no analytical results for 3D Casson fluid flow. In this manuscript, the coupled nonlinear equations are solved using Homotopy analysis method [9-11]. Analytical results are compared with Previous result [1]. Moreover analytical solution of Skin friction Co-efficient and local Nusselt number are given. In the HAM, the auxiliary parameter h converge the obtained analytical solution. Differential sensitivity analysis are graphically represented for different parameters. It shows that the behaviors of each of the parameter.

## 2. MATHEMATICAL FORMULATION AND ANALYSIS OF THE PROBLEM

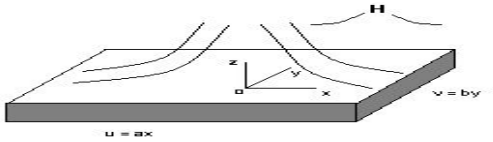


Fig.1: Physical model and coordinate [1]

The conservation equation of Continuity, momentum and energy equation is as follows [1]:

$$\frac{\partial u}{\partial x}+\frac{\partial u}{\partial y}+\frac{\partial u}{\partial z}=0 \quad (2.1)$$

$$u\frac{\partial u}{\partial x}+v\frac{\partial u}{\partial y}+w\frac{\partial u}{\partial z}=v\left(1+\frac{1}{\beta}\right)\frac{\partial^2 u}{\partial z^2}-\frac{\sigma B^2}{\rho}u-\frac{v}{K_p}u \quad (2.2)$$

$$u\frac{\partial v}{\partial x}+v\frac{\partial v}{\partial y}+w\frac{\partial v}{\partial z}=v\left(1+\frac{1}{\beta}\right)\frac{\partial^2 v}{\partial z^2}-\frac{\sigma B^2}{\rho}v-\frac{v}{K_p}v \quad (2.3)$$

$$u\frac{\partial T}{\partial x}+v\frac{\partial T}{\partial y}+w\frac{\partial T}{\partial z}=\left(\frac{k}{\rho c_p}+\frac{16\sigma T_\infty^3}{3\rho c_p k^*}\right)\frac{\partial^2 T}{\partial z^2} \quad (2.4)$$

where $u, v$ and $w$ denote the velocity components in the $x, y$ and $z$ – directions, respectively.
For Eqs.(2.1) – (2.4), the boundary conditions are[1]:

At $z=0$

$$u=U_w(x)=ax$$

$$v=V_w(x)=by$$

$$w=0$$

$$-K\frac{\partial T}{\partial z}=h_f(T_f-T) \quad (2.5)$$

At $z\to\infty$

$$u\to 0$$

$$v\to 0$$

$$T\to T_\infty \quad (2.6)$$

We introduce the similarity transformations [1]:

$$u=axf'(\eta),\ v=byg'(\eta),\ w=-\sqrt{av}\,[f(\eta)+cg(\eta)],\ \eta=\sqrt{\frac{a}{v}}\,z,\quad \theta(\eta)=\frac{T-T_\infty}{T_f-T_\infty} \quad (2.7)$$

By using Eq.(2.7), Eq.(2.1) is clearly satisfied and Eqs.(2.2) to (2.6) become [1]:

$$\left(1+\frac{1}{\beta}\right)f'''-(f')^2-(f+cg)f''-(M^2+\lambda)f'=0 \quad (2.8)$$

$$\left(1+\frac{1}{\beta}\right)g'''-(g')^2-(f+cg)g''-(M^2+\lambda)g'=0 \quad (2.9)$$

$$(1+R)\theta''+P_r(f+cg)\theta'=0 \quad (2.10)$$

where $M^2=\frac{\sigma B_0^2}{\rho a}$ is the magnetic parameter, $P_r=\frac{\rho v c_p}{k}$ is the Prandtl number, $\lambda=\frac{v}{ak_p}$ is the porosity parameter, $R=\frac{16\sigma T_\infty^3}{3kk^*}$ is the radiation parameter, $B_i=\frac{h_f}{k}\left(\sqrt{\frac{v}{a}}\right)$ is the Biot number and $c=b/a$ is the stretching parameter.

The boundary conditions are

$$\eta=0:\ f(0)=0, g(0)=0, f'(0)=1, g'(0)=c, \theta'(0)=-B_i(1-\theta(0)) \quad (2.11)$$

$$\eta=\infty:\ f'(\infty)=0, g'(\infty)=0, \theta(\infty)=0 \quad (2.12)$$

## 3. USING HOMOTOPY ANALYSIS METHOD (HAM) ANALYTICAL EXPRESSION OF VELOCITIES AND TEMPERATURE

The homotopy analysis method is a semi-analytical technique to solve nonlinear problems. This method was introduced by Liao [12]. The basic concept of this method [13,14]. Using the HAM, the approximate analytical expressions are given as follows:

$$f(\eta)=\frac{1}{\sqrt{s}}\left(1-e^{-\sqrt{s}\,\eta}\right)+\frac{h(c^2+2)}{6s\sqrt{s}}\left[e^{-2\sqrt{s}\,\eta}-2e^{-\sqrt{s}\,\eta}+1\right]+\frac{5k(h-h^2)(M^2c^2+2M^2+\lambda c^2+2h)-h^2kc^2(10-3c^2)-3h(1+c^2)(m^2+\lambda)}{18s^2\sqrt{s}}\left[1-2e^{-\sqrt{s}\,\eta}+e^{-2\sqrt{s}\,\eta}\right]+\frac{(c^2+2)[4(h-h^2)(m^2+\lambda)-2h^2(1+c^2)]}{6s^2}\left[\frac{e^{-\sqrt{s}\,\eta}-1}{\sqrt{s}}+xe^{-\sqrt{s}\,\eta}\right]+\frac{h^2(c^2+2)(c^2+3)}{36s^2\sqrt{s}}[2-3e^{-\sqrt{s}\,\eta}+e^{-3\sqrt{s}\,\eta}] \quad (3.1)$$

$$g(\eta)=\frac{c}{\sqrt{s}}\left(1-e^{-\sqrt{s}\,\eta}\right)+\frac{h(c^3+2c)}{6s\sqrt{s}}\left[e^{-2\sqrt{s}\,\eta}-2e^{-\sqrt{s}\,\eta}+1\right]+\frac{5k(h-h^2)(M^2c^3+2M^2c+\lambda c^3+2hc)-h^2kc^3(10-3c^2)-3h(c+c^3)(m^2+\lambda)}{18s^2\sqrt{s}}\left[1-2e^{-\sqrt{s}\,\eta}+e^{-2\sqrt{s}\,\eta}\right]+\frac{(c^3+2c)[4(h-h^2)(m^2+\lambda)-2h^2(1+c^2)]}{6s^2}\left[\frac{e^{-\sqrt{s}\,\eta}-1}{\sqrt{s}}+xe^{-\sqrt{s}\,\eta}\right]+\frac{h^2c\,(c^3+2c)(c^2+3)}{36s^2\sqrt{s}}[2-3e^{-\sqrt{s}\,\eta}+e^{-3\sqrt{s}\,\eta}] \quad (3.2)$$

$$\theta(\eta)=\frac{B_i(1+R)}{G+B_i(1+R)}e^{-\left(\frac{G}{1+R}\right)\eta} \quad (3.3)$$

where $s=\frac{M^2+\lambda}{k}, k=1+\frac{1}{\beta}, G=\frac{P_r(1+c^2)}{\sqrt{s}}+\frac{h(c^2+2)(1+c)}{6s\sqrt{s}}$

## 4. ANALYTICAL EXPRESSION FOR SKIN FRICTION CO-EFFICIENT AND LOCAL NUSSELT NUMBER

The expressions for skin friction coefficient is given by [1]:

$$Re_x^{1/2}\, C_{fx} = \left(1+\frac{1}{\beta}\right) f''(0)$$

$$Re_x^{1/2}\, C_{fy} = \left(1+\frac{1}{\beta}\right) g''(0) \qquad (4.1)$$

where $C_{fx} = \frac{\tau_{wx}}{\rho u_w^2}$, $\quad C_{fy} = \frac{\tau_{wy}}{\rho u_w^2}$

$C_f$ is the skin friction, $C_{fx}$ and $C_{fy}$ are skin friction along the $x$- and $y$-directions

$\tau_{wx}$ and $\tau_{wy}$ are defined in [1]

The analytical expressions for skin friction co-efficient along the $x$ and $y$ direction are represented as follows:

$$Re_x^{\frac{1}{2}}\, C_{fx} = k - \sqrt{s} - \frac{(c^2+2)[4(h-h^2)(m^2+\lambda)-2h^2(1+c^2)]}{6s\sqrt{s}} + \left\{\frac{\begin{matrix}6h(c^2+2)s+10k(h-h^2)(M^2c^2+2M^2+\lambda c^2+2h)-2h^2kc^2(10-3c^2)\\ -6h(1+c^2)(m^2+h)+3[h^2(c^2+2)(c^2+3)\end{matrix}}{18s^2}\right\}\sqrt{s} \qquad (4.2)$$

$$Re_x^{\frac{1}{2}}\, C_{fy} = k - c\sqrt{s} - \frac{c\,(c^2+2)[4(h-h^2)(m^2+\lambda)-2h^2(1+c^2)]}{6s\sqrt{s}} + \left\{\frac{\begin{matrix}6hc(c^2+2)s+10kc(h-h^2)(M^2c^2+2M^2+\lambda c^2+2h)-2h^2kc^3(10-3c^2)\\ -6h(c+c^3)(m^2+h)+[3h^2c(c^2+2)(c^2+3)]\end{matrix}}{18s^2}\right\}\sqrt{s} \qquad (4.3)$$

The dimensionless local Nusselt number is [1]:

$$Re_x^{-1/2}\, Nu = -\theta'(0) \qquad (4.4)$$

where $Re_x = u_x(x)\, x/v$ is defined in [1].

The analytical expression for local Nusselt number is

$$Re_x^{-1/2}\, Nu = -\frac{G\, B_i}{G+B_i(1+R)} \qquad (4.5)$$

where $G = \frac{P_r(1+c^2)}{\sqrt{s}} + \frac{h(c^2+2)(1+c)}{6s\sqrt{s}}$, $s = \frac{M^2+\lambda}{k}$, $k = 1+\frac{1}{\beta}$

## 5. RESULT AND DISCUSSION

Eqs.(3.1) to (3.3) represent the analytical expression of velocities and temperature. In the present section, we have discussed the velocities profile and temperature for various values of physical parameters $M, \lambda, \beta, B_i, P_r, R, C$. The well known Homotopy analysis method (HAM) is used to solve system of coupled similar Eqs. (2.8) to (2.10). The obtained analytical results are compared with the previous and numerical result in **Figs.** 2 to 12 for different values of parameters. It gives good agreement with the previous result and numerical result [1].

The velocity of the fluid for different parameters are presented in the graphs **Figs.**2 to 9. **Fig.**2 shows the influence of the velocity $f'(\eta)$ decreases with increases of casson parameter $\beta$. From **Fig.**3, it is inferred that the velocity decreases with increases of parameter. **Fig.**4 and 5 have been plotted to demonstrate the effects of parameters M and C on the velocity profiles. It is depicted that as M and C increases the velocity $f'(\eta)$ of the fluid decreases. In **Fig.**6 and 7, depict to analyze the velocity profile for various values $\beta$ and $\lambda$ . It is noticed that the $g'(\eta)$ increases with decreases of $\beta$ and $\lambda$ parameter. **Fig.**8 and 9 are displayed to show the influence of M and C on the velocity profiles. It is observed that as M increases the velocity $g'(\eta)$ of the fluid decreases. It is clear that the velocity $g'(\eta)$ increases with increases of the parameter C. The temperature of the different parameters are presented through **Figs.**10 to 12**.** From **Fig.**10, It is depicted to examine the effects of $P_r$ with temperature. It is clear that the temperature $\theta(\eta)$ decreases with increases of the parameter $P_r$. In **Fig.**11, It is revealed that the influence of temperature profile for various values $B_i$. This is because the temperature $\theta(\eta)$ increases with also increases of the parameter $B_i$. From **Fig.**12 It is clear that the parameter R increases with temperature $\theta(\eta)$ also increases.

The skin friction co-efficient and local Nusselt number are presented in **Figs.**13 to 15. From **Fig.**13, There is prominent that the skin friction co-efficient in $x$ direction increases when M also increases. It is noticed that when C increases the skin friction co-efficient $x$ direction decreases. In **Fig.**14, It illustrate that the skin friction co-efficient $y$ direction increases when the parameters M and C also increases. From **Fig.**15, Indicated the local Nusselt number decreases when M increases. It is evident that the parameter C increases with local Nusselt number also increases.

**Determining the validity region of h**

Eqs.(3.1) and (3.2) contains so called convergence control auxiliary parameter h. It plays a vital role for converging the solution series. In order to obtain the h region, the analytical solution is independent of h. To study the influence of h on the convergence of solution, the h curves of f and g are plotted in **Fig.**16. This figure clearly indicates that the valid region of h is about ( – 0.1 ).

**Differential Sensitivity Analysis**

Eq.(3.1) represent the new approximate analytical expression for the fluid $f$ in terms of the parameters $M$, $C$, $\beta$, $\lambda$ differentiating the fluid partially with respect to determined. The percentage of change in fluid with respect to $M$, $C$, $\beta$, $\lambda$ are 5.28%, 0%, 87.69%, 8.83% respectively. From this, it is evident that parameter $\beta$ have more impact on fluid. These parameter are highly sensitive parameter. The parameter $\lambda$ is called as moderately sensitive parameter as it has 8.83% of influence over fluid . The remaining two parameters M and C are less sensitive and zero sensitives. The spread sheet analysis of these result is described in **Fig.**17.

Eq.(3.2) represent the approximate analytical expression for the fluid $g$ in terms of the parameters $M$, $C$, $\beta$, $\lambda$ differentiating the fluid partially with respect to determined. The percentage of change in fluid with respect to $M$, $C$, $\beta$, $\lambda$ are 5.06%, 18.18%, 69.99%, 7.54% respectively. From this, it is inferred that parameter $\beta$ have high impact on fluid. These parameter are greatest sensitive parameter. The parameter C is called as moderately sensitive parameter as it has 18.18% of influence over fluid . The remaining two parameters M and $\lambda$ are lowest sensitive. The fluid analysis of these result is described in **Fig.**18.

Eq.(3.3) represent the approximate analytical expression for the temperature $\theta$ in terms of the parameters $M$, $C$, $\beta$, $\lambda$, $P_r$, $B_i$, $R$ differentiating the temperature partially with respect to determined. The percentage of change in temperature with respect to $M, C$, $\beta$, $\lambda$, $P_r$, $B_i$, $R$ are 82.92%, 0%, 124.37%, 20.73%, 0%, 1.95%, 141.82% respectively. From this, it is revealed that parameter R have sorely impact on temperature. These parameter are biggest sensitive parameter. The parameter $\beta$ is called as nearest sensitive parameter as it has 124.37% of influence over temperature. The parameter M is said to center sensitive parameter as it has 82.92% of examine over temperature. The remaining four parameters $\lambda$, $B_i$ and $C$, $P_r$ are smallest and zero sensitives. The temperature analysis of these result is described in **Fig.**18.

## 6. CONCLUSION

In this paper, we have investigated Analytical solution of Velocities and Temperature fields using Homotopy Analysis Method. By introducing the similarity transformation we have solved the coupled differential equations using Homotopy analysis method (HAM). We compare the present result with the numerical result and previous result, we get a very good agreement. Moreover, effects for various values of emerging parameters are discussed for velocities $f'(\eta)$, $g'(\eta)$ and temperature $\theta(\eta)$. The magnitude of the skin friction coefficients in both $x$ and $y$-directions are obtained. It is demonstrated that the obtained results are in good agreement with numerical result and previous result [1].

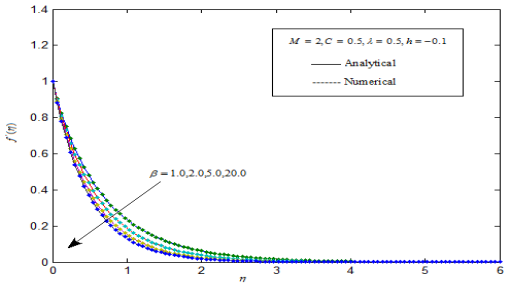


Fig.2: Plot of dimensionless velocity $f'(\eta)$ various $\eta$ at different values of $\beta$

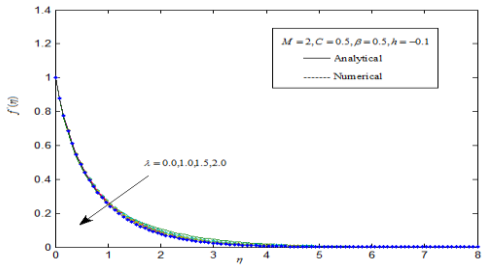


Fig.3: Plot of dimensionless velocity $f'(\eta)$ various $\eta$ at different values of $\lambda$

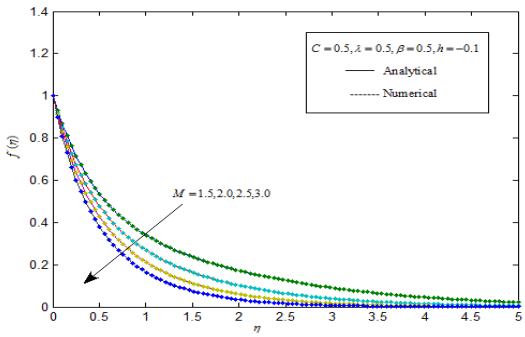


Fig.4: Plot of dimensionless velocity $f'(\eta)$ various $\eta$ at different values of $M$

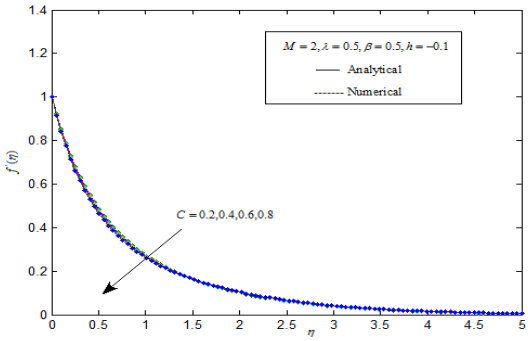


Fig.5: Plot of dimensionless velocity $f'(\eta)$ various $\eta$ at different values of $C$

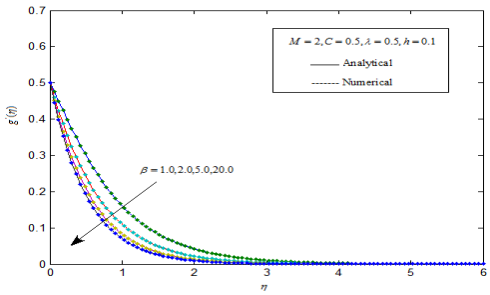


Fig.6: Plot of dimensionless velocity $g'(\eta)$ various $\eta$ at different values of $\beta$

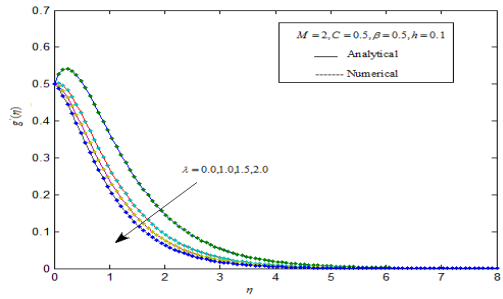


Fig.7: Plot of dimensionless velocity $g'(\eta)$ various $\eta$ at different values of $\lambda$

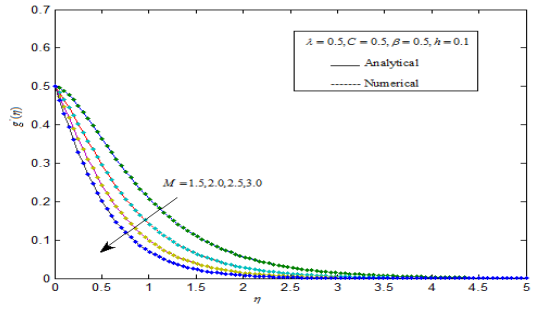


Fig.8: Plot of dimensionless velocity $g'(\eta)$ various $\eta$ at different values of $M$

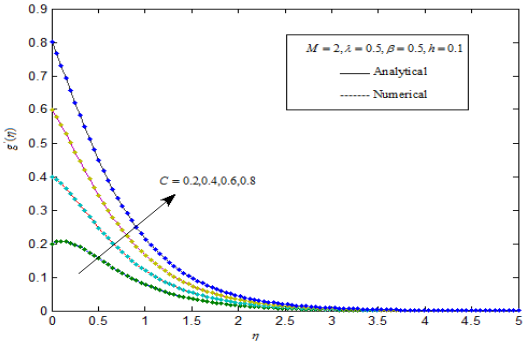


Fig.9: Plot of dimensionless velocity $g'(\eta)$ various $\eta$ at different values of $C$

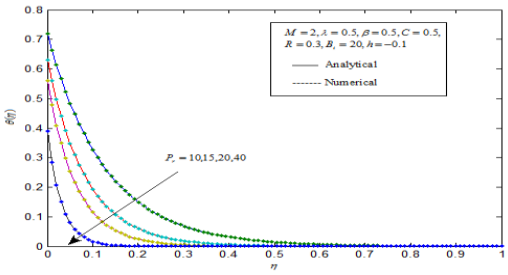


Fig.10: Plot of dimensionless temperature $\theta(\eta)$ various $\eta$ at different values of $P_r$

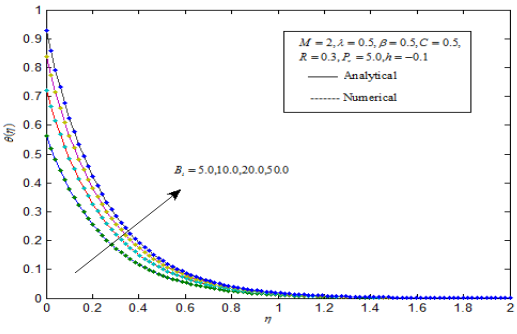


Fig.11: Plot of dimensionless temperature $\theta(\eta)$ various $\eta$ at different values of $B_i$

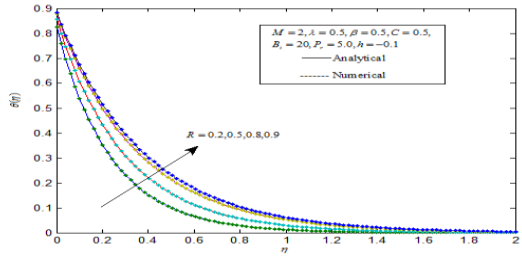


Fig.12: Plot of dimensionless temperature $\theta(\eta)$ various $\eta$ at different values of $R$

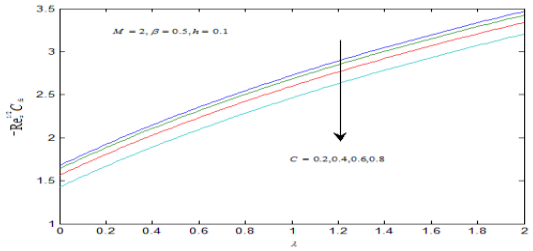


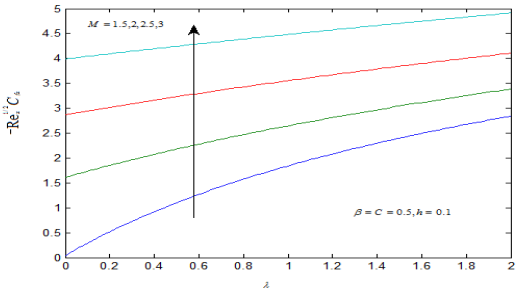


Fig.13: The graph of skin friction coefficient $Re_x^{1/2}\, C_{fx}$ for various physical parameters.

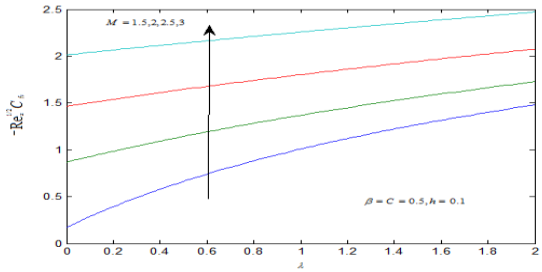


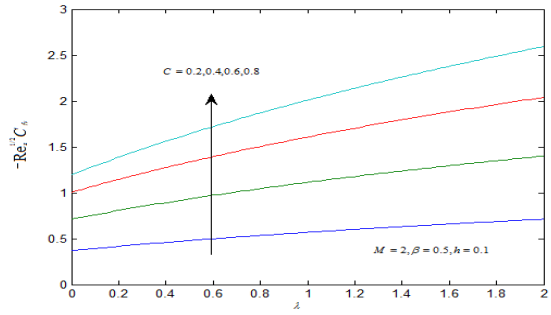


Fig.14: The graph of skin friction coefficient $Re_x^{1/2}\, C_{fy}$ for various physical parameters.

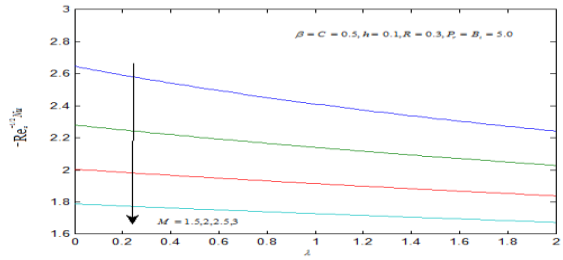

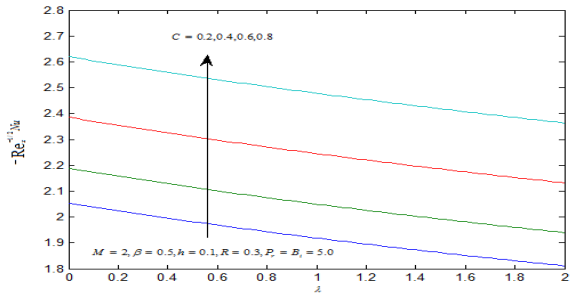


Fig.15: The graph of local Nusselt number $Re_x^{-1/2}\,Nu$ for various physical parameters.

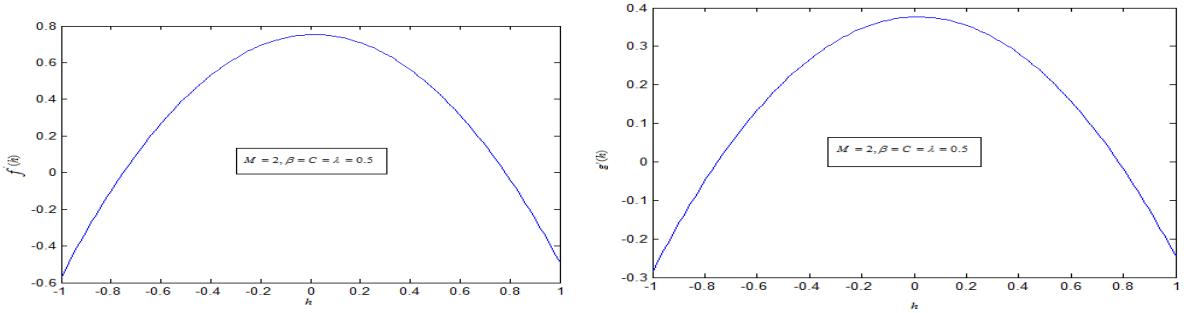


Fig.16: Validity region of $h$ curve of $f$ and $g$.

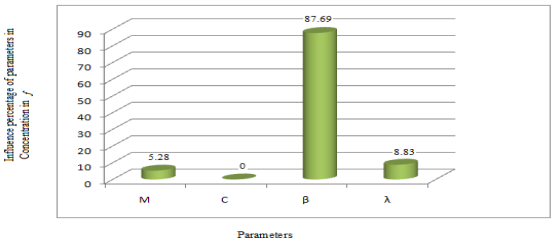


Fig.17: Sensitivity analysis for evaluating the influence of the concentration of fluid distribution in Eq.(3.1).

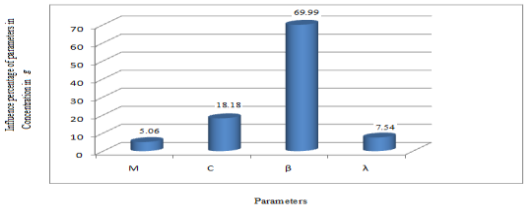


Fig.18: Sensitivity analysis for evaluating the influence of the concentration of fluid distribution in Eq.(3.2).

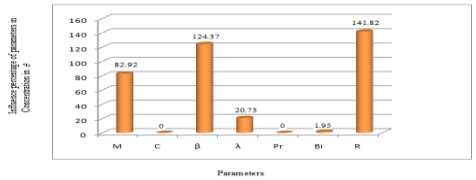


Fig.19: Sensitivity analysis for evaluating the influence of the concentration of temperature distribution in Eq.(3.3).

## NOMENCLATURE

| Parameters | Description |
|---|---|
| β | Casson fluid parameter |
| B | Magnetic |
| T | Fluid temperature |
| ν | Kinematic viscosity |

| | |
|---|---|
| $K_p$ | Permeability |
| k | Thermal conductivity |
| ρ | Density of the fluid |
| $c_p$ | Heat capacitance |
| $M^2$ | Magnetic parameter |
| λ | Porosity parameter |
| Pr | Prandtl number |
| R | Radiation parameter |
| Bi | Biot number |
| c | Stretching parameter |
| u, v, w | Velocity components along x, y and z directions |
| $U_w$ and $V_w$ | Stretching velocities in the x and y directions |
| $h_f$ | Convective heat transfer coefficient |
| $T_f$ | Convective fluid temperature |
| $C_f$ | Skin friction |
| $C_{fx}$ and $C_{fy}$ | Skin friction along the x and y directions |
| $\tau_{wx}$ and $\tau_{wy}$ | Wall shear stress along x and y directions |
| $Re_x$ | Local Reynolds number |

## APPENDIX B

## Using MATLAB program numerical solution of Eqs.(2.8)-(2.10).

```
function sol = ex8
ex8init=bvpinit (linspace(0,8,8),
[0 1 0 0 0.5 0 -2.5 0]);
sol= bvp4c(@ex8ode,@ex8bc,ex8init);
end
function dydx = ex8ode(x,y)
N=1.0;
p=5.0;
b=0.5;
M=2;
c=0.5;
R=0.3;
dydx=[y(2)
    y(3)
((b/1+b)*(y(2)*y(2)+(y(1)+c*y(4))*y(3)+(M*M+N)*y( 2)))
    y(5)
    y(6)
((b/1+b)*(y(5)*y(5)+(y(1)+c*y(4))*y(6)+(M*M+N)*y(5)))
    y(8)
    ((-p/1+R)*(y(1)+c*y(4))*y(8))
    ];
end
function res = ex8bc(ya,yb)
c=0.5;
B=5.0;
res=[
ya(1)
ya(2)-1
yb(2)
ya(4)
ya(5)-c
yb(5)
ya(8)+B*(1-ya(7))
yb(7)
];
end
```

**The command window**

```
solution=ex8;
x=solution.x;
 y=solution.y;
 y2=solution.y(2,:);
 y5=solution.y(5,:);
 y7=solution.y(7,:);

 Plot(x,y2,'r',x,y5,'g',x,y7,'b');
```

## REFERENCES

[1] G. Mahanta, S. Shaw, 3D Casson fluid flow past a porous linearly stretching sheet with convective boundary condition. Alexandria Engineering Journal 54, 653 – 659, (2015).

[2] S.Nadeem, R.U. Haq, Noreen Sher Akbar, Z.H.Khan, MHD three-dimensional Casson fluid flow past a porous linearly stretching sheet. Alexandria Engineering Journal 52, 577 – 582, (2013).

[3] B.C. Sakiadis, Boundary layer behavior on continuous solid surface. II. Boundary layer on a continuous flat surface. Journal American Institute of Chemical Engineers. 7, 221 – 225,(1961).

[4] A.M. Salem, R. Fathy, Effects of variable properties on MHD heat and mass transfer flow near stagnation towards a stretching sheet in a porous medium with thermal radiation, Chin. Phys. B. 21, 054701,(2012).

[5] S. Shaw, P.K. Kameswaran, P. Sibanda, Homogeneous- heterogeneous reactions in micropolar fluid flow from a

permeable stretching or shrinking sheet in a porous medium, Bound. Value Probl. 77,1–10, (2013).
[6] S. Nadeem , S. Zaheer, T. Fang, Effects of thermal radiation on the boundary layer flow of a Jeffrey fluid over an exponentially, Numerical Algorithms 57, 187 – 205, (2011).
[7] S. Nadeem, R.U. Haq, C. Lee, MHD flow of a Casson fluid over an exponentially shrinking sheet. Scientia Iranica 19, 550 – 553, (2012).
[8] R. Angel joy, J. Visuvasam, V.Rajendran and L.Rajendran, Theoretical Analysis of flow of nanofluid over a stretching surface, International Journal of Mathematical Archive 9 (1), 95 – 112,(2018).
[9] S. Abbasbandy, The application of the homotopy analysis method to nonlinear equations Arising in heat transfer. phys. Lett.A 360,109 –113, (2006).
[10] G. Domairry and M. Fazeli, Homotopy Analysis Method to Determine the Fin Efficiency of Convective Straight Fins with Temperature-Dependent Thermal Conductivity, Communications in Nonlinear Science and Numerical Simulation, 14 (2),489 – 499, (2009).
[11] S. J. Liao, Notes on the Homotopy Analysis Method: Some Definitions and Theorems,Communications in Nonlinear Science and Numerical Simulation, 14 (4), 983 – 997, (2009).
[12] S. J. Liao, On the Homotopy Analysis Method for Nonlinear Problems, Applied Mathematics and Computation, 147 (2), 499 – 513, (2004).
[13] S. Nadeem, S. Saleem, Analytical study of rotating Non- newtonian Nanofluid on a rotating cone, Journal of thermophysics and Heat transfer, 28 (2), 295 – 304, (2014).
[14] S. Abbasbandy, E. Magyari, E. Shivanian, The homotopy analysis method for multiple solutions of nonlinear boundary value problems, Communications is nonlinear science and numerical simulation, 14 (9), 3530 – 3536, (2009).